# Pattern Formation in Homogeneous Reactor Models

**Moshe Sheintuch and Olga Nekhamkina**
Dept. of Chemical Engineering, Technion, Israel Institute of Technology, Haifa, Israel 3200

*This work analyzes pattern formation mechanisms in the homogeneous model of a fixed catalytic bed for reactions with oscillatory kinetics. Two cases are analyzed: a nonadiabatic reactor with a continuous mass-supply (either by a preceding reaction or via a membrane wall), and a simple adiabatic or cooled reactor. In the former case, the system may reach asymptotic space-independent solutions, and when bistability of such solutions exists fronts may be established. Stationary or oscillatory front solutions, oscillatory states that sweep the whole surface, or excitation fronts may be realized then and the reactor behavior can be predicted from the sequence of phase planes spanned by the reactor. In an adiabatic reactor, fronts are formed only for sufficiently small Pe numbers, but these frontlike solutions do not separate different steady states. The patterns that can be realized in this case are quite similar to those in the previous case. The reactor behavior can be predicted by the sequence of phase planes spanned by the reactor, using an approximate finite difference presentation.*

## Introduction

The purpose of this article is to analyze pattern formation in homogeneous reactor models, using a realistic oscillatory kinetics model, and to contrast them with pattern-forming mechanisms in heterogeneous models. Patterns are formed by the interaction between front motion, fluid-flow, and changing activity. Characterizing these patterns requires understanding conditions that induce front motion and characterizing the dynamic state (phase plane) of the reactor. Fronts in homogeneous and heterogeneous reactor models emerge due to somewhat different terms (see below) making this distinction between models of catalytic beds an important point in understanding this behavior. Mechanisms of pattern formation in heterogeneous models were the subject of a recent investigation and review by Barto and Sheintuch (1994) and Sheintuch and Shvartsman (1996).

Propagating front solutions emerges in a *bistable medium* with uniform properties (i.e., with infinite convection) due to heat conduction or diffusion. Due to symmetry we may find two front solutions that propagate either to the left or to the right. The heterogeneous reactor model may admit local bistability due to the interaction of nonlinear kinetics (due to its exothermicisity or self-inhibition) with mass- or heat-transfer resistance. The fluid conditions vary along the bed and the symmetry is lost, but under certain conditions (sufficiently large flow rates) we may still find fronts moving upstream or downstream, yet at somewhat different velocities. The interaction between the fluid flow and front motion produces an array of spatiotemporal patterns (Sheintuch and Shvartsman, 1996). The homogeneous model of an adiabatic reactor typically does not admit local bistability (see below) and, strictly speaking, fronts do not exist. The interaction of flow and dispersion terms, however, creates front-like solutions and these may move in response to feed conditions or follow changes in activity. The elucidation of such patterns is one objective of this work. Fronts that separate different states may also emerge in a nonadiabatic bed with a continuous reactant supply along the bed, either by a preceding reaction or via a membrane wall. In that case the system may reach asymptotic space-independent solutions, and when bistability of such solutions exists fronts and patterns may be established, as we show below. Aside from enriching the class of solutions, feed distribution along a packed bed is an optimal solution for reactions that exhibit a local maximal rate. The recently suggested mechanism of pattern formation due

Correspondence concerning this article should be addressed to M. Sheintuch.

to the differential-flow-induced chemical instability (DIFICI; Rovinsky and Menzinger, 1992) can be interpreted in terms of a homogeneous model, and is another source of stability in catalytic beds.

Another purpose of this work is to extend the study of catalytic reactor dynamics into new cases that were not previously analyzed. We employ a simple exothermic reaction with positive-order kinetics as a source of instability. To obtain oscillatory behavior we couple the preceding reaction with a slow reversible process of changes in catalytic activity. This mechanism, in which the temperature provides the positive feedback as well as the means of communication, agrees with our current understanding of high-pressure catalytic oscillators; it was justified and was employed elsewhere to describe spatiotemporal patterns in a catalytic wire and a heterogeneous fixed-bed model (Sheintuch, 1989; Barto and Sheintuch, 1994; Middya et al., 1993).

The novelty of this work lies in the analysis of conditions for the existence of spatiotemporal patterns and their simulations in a homogeneous model of a packed-bed catalytic reactor, using realistic oscillatory kinetics. Such an analysis is more complex in a homogeneous model than in a heterogeneous one, in which local bistability emerges naturally. We also compare four classes of models that admit spatiotemporal patterns: patterns admitted by the two classes of the homogeneous model, with or without mass supply and heat removal, that are the subject of this work are compared with patterns in a heterogeneous model and with patterns possible in a simple uniform system (i.e., in the absence of convection).

The CSTR asymptote of the homogeneous axial dispersion model has been known to exhibit steady-state multiplicity and oscillatory behavior for many years now, while the PFR model cannot predict these behaviors. Bistability or oscillatory behavior due to axial dispersion was a subject of extensive investigation in the 1970s and 1980s (see Balakotayah, 1996; Subramanian and Balakotayah, 1996, and references therein). It requires a sufficiently large ratio of axial diffusion to convection terms (small $Pe_c = u_s Z/D_e$), and several reviews of this topic are available (Hlavacek and Van Rompay, 1981). It is currently believed that this model cannot account for observations of catalytic oscillations, since instabilities have been observed on a single crystal, pellet, or wire even in the absence of interaction with the gas phase. Furthermore, for reasonable values of parameters the axial dispersion model predicts oscillations that are much faster than those observed experimentally.

The structure of this work is as follows: The homogeneous reactor model is presented in the next section and its asymptotic cases are noted. The full model, accounting for mass supply and heat loss through the wall, is discussed in the third section, as it admits real fronts that separate domains of different solutions and known mathematical results can be applied then. In the last section we study motions of the more realistic case of adiabatic or cooled reactors. In each case we study the motion qualitatively, by tracking it on the phase plane of the system, and support it by simulations of first-order exothermic reaction with a large *Pe* number. Patterns in the heterogeneous model are briefly discussed in the concluding remarks, mainly to contrast them with those of the homogeneous model.

## Homogeneous Model

Typical homogeneous models account for mass and energy balances with accumulation, flow, and axial dispersion terms along with chemical reaction and heat loss due to cooling $[S_T = HP(T - T_w)]$, subject to the Danckwert's boundary conditions. To demonstrate some of the possible motions we also incorporate a mass generation source $(S_C)$, either by a preceding reaction or by mass supply through a membrane wall or via many stages of interstaged-feeding:

$$\epsilon \frac{\partial C_A}{\partial t} + u_s \frac{\partial C_A}{\partial z} - D_e \frac{\partial^2 C_A}{\partial^2 z} = -(1-\epsilon) r(C_A, T, \theta) + S_C \tag{1}$$

$$(1-\epsilon)\rho_s c_{ps} \frac{\partial T}{\partial t} + u_s \rho c_{pf} \frac{\partial T}{\partial z} - k_e \frac{\partial^2 T}{\partial^2 z}$$
$$= (-\Delta H)(1-\epsilon) r(C_A, T, \theta) - S_T \equiv Q^* f(C_A, T, \theta) \tag{2}$$

$$u_s \rho c_{pf}(T_{\text{in}} - T|_0) = -k_e \left.\frac{\partial T}{\partial z}\right|_0; \qquad \left.\frac{\partial T}{\partial z}\right|_L = 0;$$

$$u_s(C_{A\text{in}} - C_A|_0) = -D_e \left.\frac{\partial C_A}{\partial z}\right|_0; \qquad \left.\frac{\partial C_A}{\partial z}\right|_L = 0. \tag{3}$$

We use conventional notation in Eqs. 1–3, and $Q^*$ is the characteristic specific heat-generation term. We have also neglected the fluid heat capacity in the accumulation term. We will limit our discussion to exothermic reactions of positive-order kinetics, a situation known to exhibit bistability in a CSTR, and to such reactions coupled with slow reversible changes in catalytic activity $(\theta)$.

The physical interpretation of the slow activation and deactivation steps, which lead to oscillations, is rather wide and must be specified for each particular reaction and catalyst: at low pressures the low and localized process of surface modification takes the form of surface reconstruction or subsurface oxygen penetration (see review by Imbihl and Ertl, 1995). Subsurface oxygen formation was shown to occur also on a surface of polycrystalline catalysts under low- and high-pressure conditions. Many oxide- and metal-catalyzed high-pressure oxidation reactions are believed to oscillate due to oxidation and reduction of its surface (e.g., see review by Schuth et al., 1993, and the monograph by Slinko and Jaeger, 1994). The fraction of the active surface area $(\theta)$ is nondiffusing and the general form of its balance is

$$\tau_\theta \frac{\partial \theta}{\partial t} = g(T, \theta). \tag{4}$$

This is a slow process and its time scale $(\tau_\theta)$, which can be estimated from the period of oscillations (10 to $10^4$s), is much larger than the enthalpy-balance time scale $(\tau_T)$. We adopt here a simple linear expression for $g(T,\theta)$ (see Barto and Sheintuch, 1994, for justification), that assumes that deactivation occurs faster at higher temperatures and at higher activities, and that it is independent of reactant concentration, so that it can be expressed by a single line in the $(T,\theta)$ phase

plane:

$$\frac{\partial\theta}{\partial t} = -\left[k_{d-} + \mu(T - T_{\text{in}})\right]\theta + \left[k_{d+} - \mu(T - T_{\text{in}})\right](1-\theta). \tag{5}$$

We distinguish between three situations of the mass-source and heat-loss terms:

(1) With continuous mass supply ($S_C > 0$), and in a cooled reactor, the system may admit asymptotic homogeneous (space-independent) solution(s), $C_{As}$ and $T_s$, that satisfies the righthand side of Eqs. 1 and 2. This problem is convenient for analysis, since when two stable space-independent solutions exist we can imagine a front that separates two domains where the upper or lower solution exists. These domains may be almost homogeneous and boundary effects will be evident only near the inlet. The temperature profile may now exhibit several hot and cold domains, as we can produce several such fronts in the reactor. (2) In a tubular reactor without reactant supply but with cooling at the wall, that is, when $S_C = 0$ and $S_T = HP(T - T_w)$, the temperature profile may exhibit a local maximum but instabilities may be induced by strong axial conduction. (3) An adiabatic bed with an impermeable wall will exhibit a monotonically increasing temperature profile, and again instabilities may be induced by strong conduction.

The emerging spatiotemporal patterns are described in the next sections, for the three preceding situations, after we review the relevant results of dynamics of convectionreaction systems.

## Pattern Formation in Systems with Mass-Source and Heat-Loss

When cooling and mass supply, as well as conduction, are accounted for, the system may admit traveling fronts connecting different steady states. The concentration and temperature profiles need not be monotonic. The reactor may achieve an asymptotic homogeneous solution, toward the reactor outlet, that satisfies the righthand side of Eqs. 1 and 2. If many such solutions can exist, then fronts can be induced.

If the reactant supply term obeys $S_C = H_c P(C_W - C_A)$, as in a transfer through a membrane wall, then the steady-state fixed-$\theta$ solution of $r(C_{As},T_s) = H_c P(C_W - C_{As})/(1-\epsilon) = HP(T_s - T_w)/[(1-\epsilon)(-\Delta H)]$ can be analyzed as in the familiar CSTR problem by finding the linear relation between $T_s$ and $C_{As}$ and substituting it into $r(C_{As},T_s)$ to form the sigmoidal heat-generation curve $Q_g(T_s;C_W,T_W)$. Its intersection with the cooling heat-removal lines may admit three solutions $T^{(i)}$, $i = 1$, 2, or 3. Near the reactor exit the system attains one of the stable homogeneous solutions, $T^{(1)}$ or $T^{(3)}$. At the inlet there will be an entrance zone where $T$ varies from a value close to $T_{\text{in}}$ toward one of these solutions; the choice of the stable state depends on inlet and initial conditions.

### *Front motion (fixed $\theta$)*

Fronts separating the hot and cold states can be induced sufficiently far from the entrance zone. A reactor that asymptotically approaches the hot state can be perturbed at the outlet to the cold state. We now analyze the fate of such a front in a constant-activity system (fixed $\theta$), and then proceed to study the dynamics with changing activity. The problem can be cast now in an inner–outer solution formalism. Away from the front the conductivity terms can be ignored. To simplify the analysis and convert the problem into a single-variable problem, we assume that $T$ and $C_A$ are related at every position. The inner solution obeys

$$(1-\epsilon)\rho c_{ps}\frac{\partial T}{\partial t} + u_s \rho c_{pf}\frac{\partial T}{\partial z} - k_e\frac{\partial^2 T}{\partial^2 z} = Q_g(T;C_W) - HP(T - T_w)$$

$$T(-\infty,t) = T^{(3)}; \qquad T(\infty,t) = T^{(1)}. \tag{6}$$

This problem is similar to the well-known problem of a traveling front in a reaction-diffusion system, except that now there is a convection term as well. The solution is quite similar also: a front moving at a constant speed ($V$) and shape. To show that, set Eq. 6 in the frame of a coordinate moving with the front, $\zeta = z - Vt$, to find

$$-V(1-\epsilon)\rho c_{ps}\frac{dT}{d\zeta} + u_s \rho c_{pf}\frac{dT}{d\zeta} - k_e\frac{d^2 T}{\partial\zeta^2} = Q_g(T;C_w) - HP(T - T_w) \equiv Q^* f(T;C_w,T_w). \tag{7}$$

Certain results and properties of the front velocity ($V_{u=0}$) in conduction-reaction single-variable systems like Eq. 7 ($u_s = 0$) were reviewed by Fife (1979) and Mikhailov (1990): analytical solutions exist only in few cases, like a cubic or a step (Heaviside) $Q_g(T)$ function; several approximate solutions were suggested (e.g., see Sheintuch and Shvartsman, 1996). The front becomes stationary ($V = 0$) only for a certain set of parameters that obey $\int f(T;C_w,T_w)dT = 0$, when integrated between the stable steady states $T^{(1)}$ and $T^{(3)}$; conditions between this boundary and the ignition (extinction) points lead to expansion of the hot (cold) zone. To account for convection the front velocity should be modified by

$$V = V_{u=0} - U \tag{8}$$

with $U$ defined by

$$U \equiv \frac{u_s \rho c_{pf}}{(1-\epsilon)\rho_s c_{ps}}. \tag{9}$$

Positive or negative $V_{u=0}$ implies an upstream- or downstream-moving front, respectively. Applying this results to the convection–conduction–reaction problem, we find that the front velocity has a strong bias for motion in the downstream direction: the velocity of upstream-moving fronts varies monotonically between $V_+ - U$ and $V_- - U$, where $V_\pm$ are the extreme front velocities in the absence of convection, those at the boundaries of the bistability domain. A stationary solution may emerge only if $U < V_+$; otherwise, all fronts propagation downstream. These results apply for a front that is

placed at will at any position of the reactor, but the entrance zone may affect this behavior if the front is sufficiently close to the inlet. Fronts propagating downstream move fast at a velocity between $V_+ + U$ and $V_- + U$.

Recall that $U$, which is proportional to the interstitial velocity and to the ratio of fluid to solid heat capacity, is the velocity of perturbations traveling in a single-variable reaction-convection system (Eq. 2 with $k_e = 0$, assuming also that $C_A$ and $T$ are related everywhere). Before proceeding we comment about the properties of such reaction–convection models: obviously such a model, in which perturbations always travel downstream, cannot induce instabilities, but fluctuations or oscillations induced at the inlet can be amplified significantly, since $f(T,C_A)$ is highly nonlinear. Periodic perturbations at the inlet will convert at the outlet to high-temperature oscillations with a similar frequency. This may account for the observations of Wicke and Onken (1988) during CO oxidation in a fixed bed. Typically $C_A$ and $T$ are not explicitly related as perturbations in concentration move faster than those of enthalpy, inducing effects like wrong-way behavior (see a review by Luss, 1997), but that will not affect the preceding conclusion.

### *Phase plane analysis (varying $\theta$)*

The problem becomes much more complex when reversible changes in catalytic activity are accounted for. If we assume again that $C_A$ and $T$ are related, then this problem is described by a two-variable model (Eqs. 2–4) where the catalyst temperature is the activator and its length scale is larger than that of the inhibitor ($\theta$), which is believed to be a slowly changing surface concentration. The motion can be interpreted in terms of the relative disposition of the null curves: $f(T,\theta) = 0$ is typically S-shaped, as it should admit bistability, while $g(T,\theta) = 0$ can be monotonic or even linear (Figure 1, plotted with dimensionless variables). The steady state of the local problem, the intersection of the $f(T,\theta) = 0$ and $g(T,\theta) = 0$ is stable when located on the upper or lower branches of $f(T,\theta) = 0$ and unstable when located on the intermediate branch and when time-scale separation is sufficiently wide. The steady state is usually classified as *excitable* when a stable steady state is located near the limit points of $f(T,\theta) = 0$, as *oscillatory* when the steady state is unstable (Figure 1, line *a*), and as *bistable* (line *b*). In the absence of convection a uniform and long one-dimensional reaction–conduction system may admit a traveling pulse or front, propagating upstream or downstream after being triggered locally, or may sustain homogeneous oscillations. Such a system is unlikely to exhibit sustained spatiotemporal patterns in the absence of gradients in properties due to convection, or nonuniformities (see Sheintuch and Shvartsman, 1996, and references therein, for a detailed review).

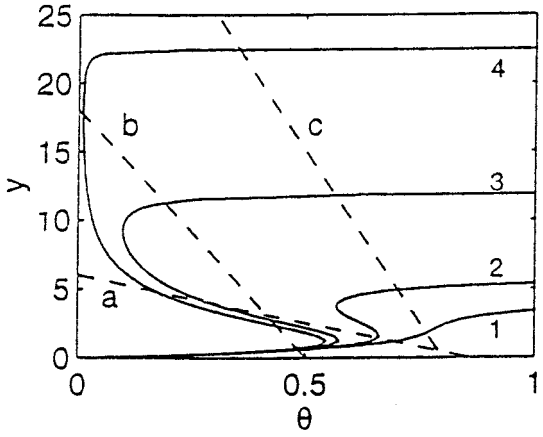


**Figure 1. Typical asymptotic phase-planes in a reactor with mass source and heat sink (such as, a cooled membrane reactor).**

It shows the enthalpy null curves [$f = 0$, solid lines, with $B = 30$, $\gamma = 20$, $Da/\alpha_T = 0.025$, $x_W = y_W = 0$, and $\alpha_C/\alpha_T = 0.15$ (line 1), 0.20 (2), 0.40 (3), and 0.75 (4)]. The activity null curves are also shown [$g = 0$, broken lines with $(K, M) = (5.67, 18.9)$, (1, 1.11) and (4, 2) for lines *a*, *b*, and *c*].

The behavior in a reactor is different due to the effect of convection: convection accelerates fronts or pulses propagating downstream and slows down or forbids upstream motion altogether. Convection will also affect the inlet boundary conditions in a way that the nature of motion there will be different from that in the rest of the system. Thus, if the system asymptotically reaches an excitable state, then its triggering at the exit may induce a slow front (if $U < |V_{u=0}|$) moving upstream, or the front may be washed out immediately (if $U > |V_{u=0}|$). In the former case, the front may be arrested somewhere inside the reactor and collide with the ensuing front. If conditions upstream induce an oscillatory motion, then it will trigger a sequence of fast fronts (at $U + |V_{u=0}|$) that sweep the oscillatory domain.

The analysis is simplified significantly in a system with periodic boundary conditions (Rovinski and Menzinger, 1993). Patterns may be realized then even in the absence of convection: Eqs. 2 and 4, while assuming a simple relation between $C_A$ and $T$, can be converted, using the transformation $\zeta = (u_s t - z)/(u_s - U)$, to

$$(1-\epsilon)\rho_s c_{ps}\frac{dT}{d\zeta} = Q^* f(T,\theta); \qquad \tau_\theta \frac{u_s}{u_s - U}\frac{d\theta}{d\zeta} = g(T,\theta). \tag{10}$$

Therefore, in the frame of the moving coordinate, the system is described by the model of the lumped system (Eqs. 2 and 4; $u_s = 0$) except that the slow time scale is modified by the ratio $u_s/(u_s - U)$. In the case of a large separation of time scales, that will not affect the solution, while with similar time scales the flow may stabilize a system that is oscillatory in the absence of flow. Patterns may be realized with the wave traveling against the flow ($U < 0$). The wave pattern is identical to the temporal oscillatory solution of the homogeneous system. The periodic boundary conditions require that the pattern velocity ($U$) be the ratio of the system length to the oscillations period (or its integer multiple). Periodic boundary conditions cannot be realized in a simple way in a tubular reactor. In a system with $\tau_T/\tau_\theta \to 0$ the pattern may be constructed analytically, similar to patterns on a ring (see Mikhailov, 1991; Middya et al., 1994). Moreover, patterns will

not emerge even in a recycle reactor, since pattern formation of the proposed mechanism requires feedback from the reactor inlet to its exit, contrary to the feedback in the recycled reactor.

### *Dimensionless equations and simulations*

To simulate the problem we present the general model for a first-order activated kinetics, $r = \theta A e^{-E/RT} C_A$, in terms of conventional notation of dimensionless parameters and variables

$$\frac{\partial x}{\partial \tau} + \frac{\partial x}{\partial \xi} - \frac{1}{Pe_C}\frac{\partial^2 x}{\partial \xi^2} = Da\theta(1-x)\exp\left(\frac{\gamma y}{\gamma + y}\right) + \alpha_C(x_w - x) = f_1(x,y,\theta)$$

$$Le\frac{\partial y}{\partial \tau} + \frac{\partial y}{\partial \xi} - \frac{1}{Pe_T}\frac{\partial^2 y}{\partial \xi^2} = B\cdot Da\theta(1-x)\exp\left(\frac{\gamma y}{\gamma + y}\right) - \alpha_T(y - y_w) = f_2(x,y,\theta)$$

$$\xi = 0, \qquad \frac{\partial x}{\partial \xi} = Pe_C x, \qquad \frac{\partial y}{\partial \xi} = Pe_T y;$$

$$\xi = 1, \qquad \frac{\partial x}{\partial \xi} = \frac{\partial y}{\partial \xi} = 0, \tag{11}$$

with

$$x = 1 - \frac{C_A}{C_{A,\text{in}}}; \qquad y = \frac{\gamma(T - T_{\text{in}})}{T_{\text{in}}}; \qquad \xi = \frac{z}{L}; \qquad \tau = \frac{tu_s}{L};$$

$$Da = \frac{Ae^{-\gamma}L}{u_s}; \qquad \gamma = \frac{E}{RT_{\text{in}}}; \qquad B = \gamma\frac{(-\Delta H)C_{A,\text{in}}}{\rho c_{pf} T_{\text{in}}};$$

$$Le = \frac{(1-\epsilon)\rho_s c_{ps}}{\rho c_{pf}}; \qquad Pe_C = \frac{Lu_s}{D_e}; \qquad Pe_T = \frac{\rho c_{pf} L u_s}{k_e};$$

$$\alpha_C = \frac{H_C PL}{u_s}; \qquad \alpha_T = \frac{H_T PL}{\rho c_{pf} u_s}. \tag{12}$$

The slow process is described by

$$\tau_\theta \frac{\partial \theta}{\partial \tau} = -\frac{M}{\gamma} y - (1+K)\theta + K \equiv g(y,\theta);$$

$$\tau_\theta = u_s/Lk_{d-}; \; K = k_{d+}/k_{d-}; \; M = \mu T_{\text{in}}/k_{d-}. \tag{13}$$

Numerical simulations of the full model were performed by an implicit finite difference scheme based on the method of fractional steps with up to 600 equidistant mesh points while verifying convergence with respect to cell size. The order of this scheme is $O(\tau^2, \Delta\xi)$. The solid temperature profiles were presented as colored contours in the position vs. time plane. The values of physicochemical constants and model parameters that were employed in the simulations are realistic for fixed-bed reactors (i.e., large *Le* and *Pe* numbers, highly exothermic and activated reactions) and typically follow the values used by Barto and Sheintuch (1994) for heterogeneous reactor models (see Appendix there-in).

To explain the possible motions we analyze the possible asymptotes in a long reactor by extracting the linear relation between and temperature and concentration, $B\alpha_C(x_W - x) = \alpha_T(y - y_W)$, obtained by setting $f_1,(x,y,\theta) = f_2(x,y,\theta) = 0$, and substituting it into $f_2 = 0$ to obtain the $f(y,\theta)$ null curve; the latter is plotted in Figure 1 for various transport coefficients and $x_W = y_W = 0$, along with $g(y,\theta) = 0$. The intersections of these null curves are the asymptotes and their nature was described earlier. The behavior at the reactor entrance is generally different from these asymptotes, as it is affected by feed conditions and boundary conditions.

*Bistable Phase-Plane and Switching.* A bistable reaction–conduction uniform system may be triggered locally, at its left or right edge or anywhere else, and the ensuing front(s) will switch the system from one state to another. Convection may affect this motion. The two stable solutions possible for a certain case, where the asymptotic behavior is bistable (Figure 1, line *b*), are plotted as lines 0 and 7 in Figures 2a, 2b: one solution shows negligible activity, while the other shows a declining temperature profile for this particular case. A local perturbation may switch the reactor from one state to another. When the reactor outlet is perturbed over a narrow zone, from the low state to a high-temperature (see line 0 in Figure 2a), a slow front is induced, and it travels upstream almost at a constant speed until the upper state is attained. A perturbation imposed on the high-temperature state at the outlet disappeared immediately (not shown), since the local ignite state is more stable (that is, the ignited state expands) and the front exits the reactor. A perturbation of the low-temperature state at the inlet propagates through the reactor and switches it to the high state (Figure 2b); a perturbation imposed at the inlet on the high state did not propagate (not shown).

*Oscillatory Phase Plane.* A typical oscillatory motion exhibits almost-homogeneous relaxation oscillations between the low-activity and high-activity branches (Figure 2c, which presents one cycle, and Figure 2d; see Figure 1, line *a* for the corresponding phase plane); the transition between these branches is fast in time, as is evident from Figures 2c and 2d; the latter represents the inlet and outlet temporal behavior.

*Other Motions.* The behavior at the inlet zone is governed mainly by the axial dispersion, as is described below in the description of nonadiabatic reactors. If that behavior produces oscillatory behavior, then it will induce successive fronts that propagate through the excitable sections of the system. For the simulations in Figure 3 the inlet produces oscillations, but the asymptotic behavior of a long reactor is stable and unexcitable (line *c* in Figure 1). For small $\alpha_C$ values the system behaves like a nonadiabatic reactor (see below) and the whole reactor oscillates between the extinguished and ignited states. For large $\alpha_C$ values the reactor reaches its asymptotic solution, which in this case is a stable unexcitable state, but the inlet zone periodically produces extinction fronts that travel through the reactor until they become stationary; by then the upstream section activates and the front turns around and becomes an ignition front.

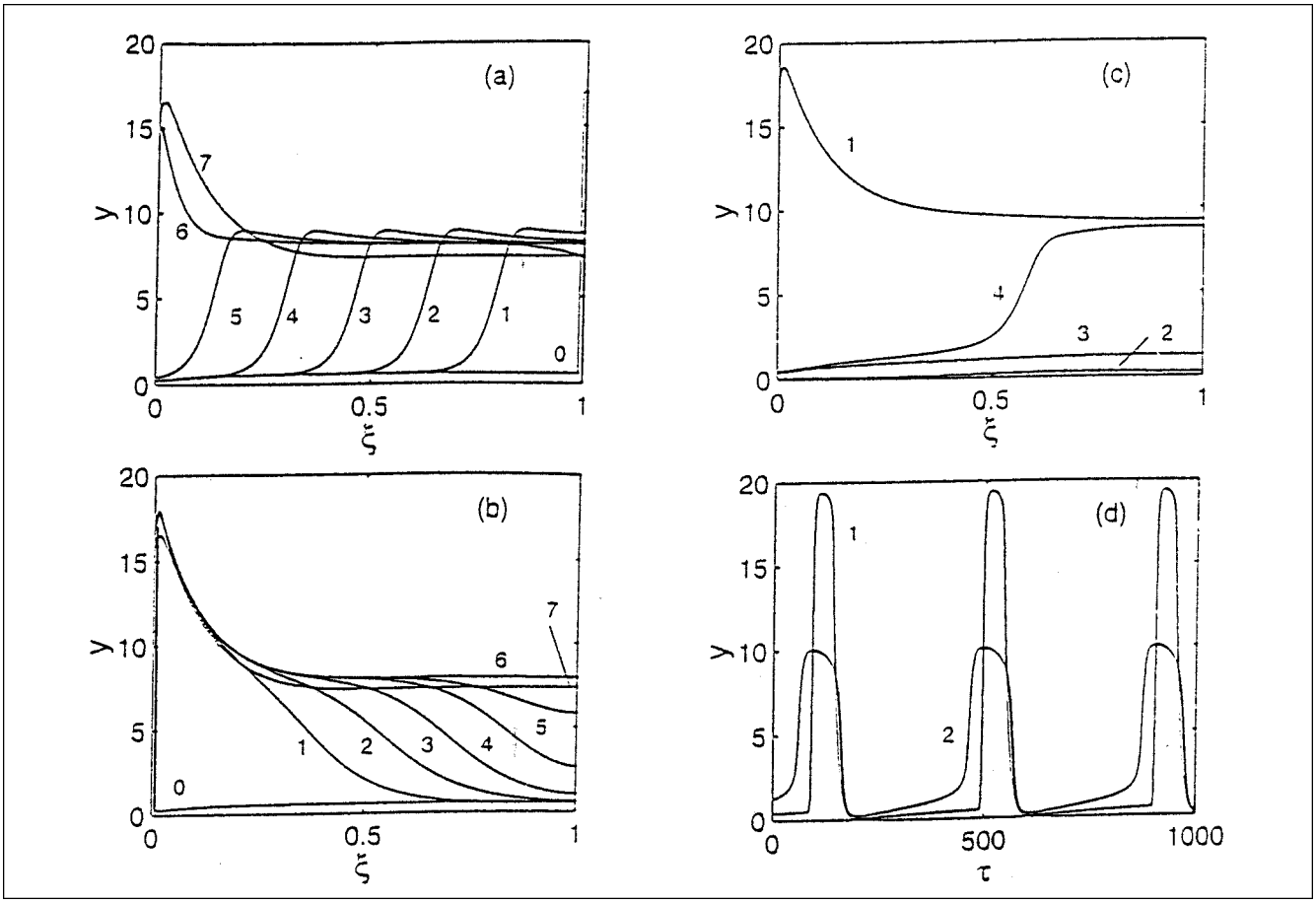


**Figure 2. Typical behaviors in a reactor with mass source and heat sink.**

(a,b) Switching from a low (line 0) to a high (line 7) steady state upon a perturbation imposed at the exit (a) or the inlet (b); (c,d) oscillatory behavior presented in the space domain (c) or in the time domain for the inlet and outlet positions (d) [$Pe_T = Pe_C/10 = 10$; $B = 30$, $\gamma = 20$, $Da/\alpha_T = 0.025$, $x_W = y_W = 0$, $Le^* = 100$, $\tau_\theta = 1000$, with $\alpha_C/\alpha_T = 0.29$ (a,b) or 0.35 (c,d), $K = 1$ and $M = 1.11$ (a,b) or 5.67 and 18.9 (c,d); lines in 0–7 are equally intervaled with $\Delta t = 10$ (a), 40 (b), or 67.5 (c; several lines are not shown)].

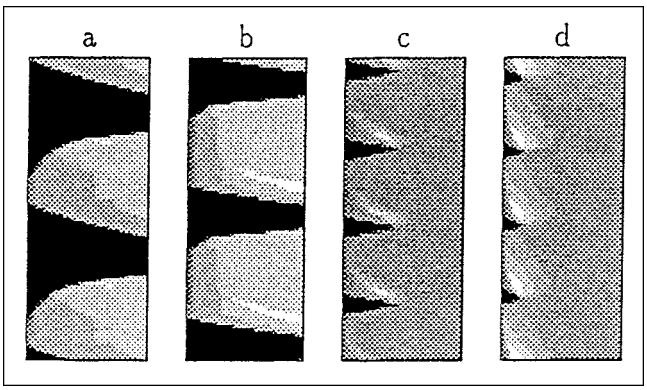


**Figure 3. Typical oscillatory behaviors in a reactor with mass source and heat sink.**

It is presented as gray-scale contours (ordinate is time, while abcissa is spatial coordinate; the reactor feed is on the left; white and black shades denote the highest and lowest temperatures). $Pe_T = 50$; $Pe_C = 5$, other parameters as in Figure 2 with $\alpha_C/\alpha_T = 1.5$ (a), 2.0 (b), 4.5 (c), and 6.0 (d), $K = 4$ and $M = 2$ (line *c* in Figure 1).

## Pattern Formation in Adiabatic ($\alpha_C = \alpha_T = 0$) and Cooled ($\alpha_C = 0$) Reactors

In the absence of a mass source the concentration profile is monotonically declining and the motions described previously cannot be realized. Instabilities can be induced due to strong axial mixing by thermal conduction. These phenomena can be realized typically in short reactors and can be viewed as an extension of instabilities in a mixed reactor. However, stationary fronts can be realized even with a small mixing term, provided the thermal feedback parameters (exothermicisity and activation energy) are sufficiently strong. Here we extend this model by adding the slow activation and deactivation processes and convert it into a simple and realistic oscillatory mechanism and solve it then for realistic high *Pe* number.

### *Phase-plane analysis*

Before turning to numerical solutions let us approximate and analyze the behavior of an adiabatic reactor in the

phase-plane by discretizing the distributed-variable problem while assuming an adiabatic relation between $C_A$ and $T$. To that end we convert Eq. 2 to the form

$$\tau_T\left(\frac{\partial T}{\partial t}+U\frac{\partial T}{\partial z}\right)-L_T^2\frac{\partial^2 T}{\partial z^2}=\Delta T_{\rm ad}\,f(T,\theta,C_A);$$

$$f=\frac{r(T,\theta,C_A)}{r_{\rm ref}};\qquad Q^*=\frac{(1-\epsilon)(-\Delta H)}{\Delta T_{\rm ad}}r_{\rm ref};$$

$$L_T^2=\frac{k_e}{Q^*};\qquad \tau_T=\frac{(1-\epsilon)\rho c_{ps}}{Q^*},\quad (15)$$

subject to boundary-conditions (Eq. 3), with a similar equation for $C_A$ (Eq. 1); $r_{\rm ref}$ is a reference rate chosen so that $f$ is of order unity and $L_T$ and $\tau_T$ have been defined with respect to $Q^*$, the characteristic heat production. Now, for fixed $\theta$ and with an adiabatic relation between $C_A$ and $T$, Eq. 15 is similar to Eq. 9 but since $f=0$ is single-valued, it *cannot* admit a front that connects two stable solutions of $f=0$; $f(T, C_A(T), \theta)$ is very small at low $T$, passes through a maximum at intermediate $T$, and intersects the abscissa at the adiabatic temperature rise. In the general case, $C_A(T)$ cannot be expressed in a simple way, but since the front motion is slow due to the large solid-phase heat capacity, the system can be assumed to be in a pseudo-steady-state and with similar mass and enthalpy dispersion terms, this relation is approximately valid. Below we derive $C_A(T)$ relations for transients in which a front propagates at a constant velocity and show that the maximal temperature exceeds the adiabatic temperature rise when a front propagates downstream.

To present the motion in the phase plane we consider the finite difference approximation of Eq. 15. A meaningful approximation will use cells that are of an order of magnitude of front width: there are two length scales in this problem, one due to conduction and heat-generation terms ($L_T$) and another due to conduction and convection terms. In the former case we can rewrite Eq. 15 in terms of a finite difference scheme that approximates the solution for cell $i$ as

$$\tau_T\frac{\partial T_i}{\partial t}-(T_{i+1}+T_{i-1}-2T_i)=\Delta T_{\rm ad}\,f(T_i,\theta_i,C_{Ai})$$
$$-\frac{U\tau_T}{L_T}(T_i-T_{i-1})\equiv F(T_i,\theta_i,C_{Ai}).\quad (16)$$

Using the other length scale, the ADM is commonly approximated by equivalence with a model of cells (mixed reactors in series), each of size $\Delta z=2L/Pe_T$ (or $=2L_T^2/U\tau_T$ in our notation), where the Peclet number is $Pe_T=u_s\rho c_p L/k_e = LU\tau_T/L_T^2$ (e.g., see Balakotaya, 1996; this result is exact for low conversion and high $Pe_T$). In that case, the cell model reads

$$\tau_T\frac{\partial T_i}{\partial t}-\left(\frac{Pe_T L_T}{2L}\right)^2(T_{i+1}+T_{i-1}-2T_i)=\Delta T_{\rm ad}\,f(T_i,\theta_i,C_{Ai})$$
$$-\frac{1}{2}\left(\frac{Pe_T L_T}{L}\right)^2(T_i-T_{i-1})\equiv F(T_i,\theta_i,C_{Ai}).\quad (17)$$

These approximations are similar to the approximations of a reaction–conduction equation, with a heat-generation and heat-removal term on the righthand side, except that the heat removal varies with position (the equations should also be modified near the inlet). When conduction is small (but its impact is evident at $L_T$) the steady-state solution can be easily determined graphically by moving the heat-removal line parallel to itself and stepping from its intersection with $\Delta T_{ad} f$ (at $T_i$) to the intercept with the abscissa for the next line. If the solution is unique for all $T_i$, then the profile is moderate and conduction may be ignored. For large conductivity (large $L_T$), and a steep $f$ (i.e., large activation energy or exothermicity) the system may acquire multiple solutions and the conduction term becomes important. A front may form then and move to a stationary position that satisfies the boundary conditions.

Let us turn now to the phase plane. If the bistability due to axial mixing is coupled with slow reversible deactivation (Eq. 4), then several cells may exhibit relaxation oscillations. To show that, we solve the dimensionless version of the steady-state thermal balance (Eq. 16) for a first-order reaction and with $x_i(C_{Ai})$ that depends adiabatically on $y_i(T_i)$, for various $\theta_i$ values, and plot it typically as a series of curves ($y_i$ vs. $\theta_i$) for various $y^*(=y_{i-1})$, in the phase plane (Figure 4). In dimensionless terms the null curves take the form of

$$B\cdot Da\theta(1-x)\exp\left(\frac{\gamma y}{\gamma+y}\right)-\frac{Pe_T}{2}(y-y^*)=F(y,\theta),\quad (18)$$

with $y=Bx$. The breadth of activities ($\theta$) that induce multiple temperatures ($y$) diminishes with increasing $Pe_T$ (three such curves are shown in Figure 4). The other null curve ($g=0$) may intersect these curves to form an excitable, oscillatory or bistable system, or may form a mixture of such characters that varies along the reactor. The system motion then depends on the nature of the phase planes spanned by the varying $y^*$ or ($T^*$); this sequence depends on the $g=0$ as well (of the two parameters in $g$, $M/\gamma$ is the slope and $K/(1+K)$ is its intersection with $y=0$). For low $M$ ($=1$ or 2) and the high $Pe_T$ number used in our simulations, the plane is either bistable or extinguished and unexcitable at low $y^*$, and as the temperature increases it shifts into a unique and ignited state. For intermediate $M$ and low $y^*$, the plane acquires three solutions, of which only the extinguished is stable, and it shifts into an oscillatory phase plane and an extinguished state with increasing $y^*$. For large $M$, the state is extinguished for all $y^*$. Note again that the assumption of an adiabatic $x(y)$ relation strictly applies only for certain conditions. Since this presentation is only an approximation, we use it in order to gain a qualitative understanding of the motion in the phase plane.

### *Front motion*

The problem of constant-pattern front motion in the ADM has been the subject of extensive investigation. Conditions for the existence of such fronts and approximations for their velocity were derived by Frank-Kamenetski (1969), Zeldovich and Barenblatt (1959), Merzhanov et al. (1973), and Wicke and Vortmayer (1959). A relevant review of the subject is presented by Puszynski et al. (1987), who analyze the ignition

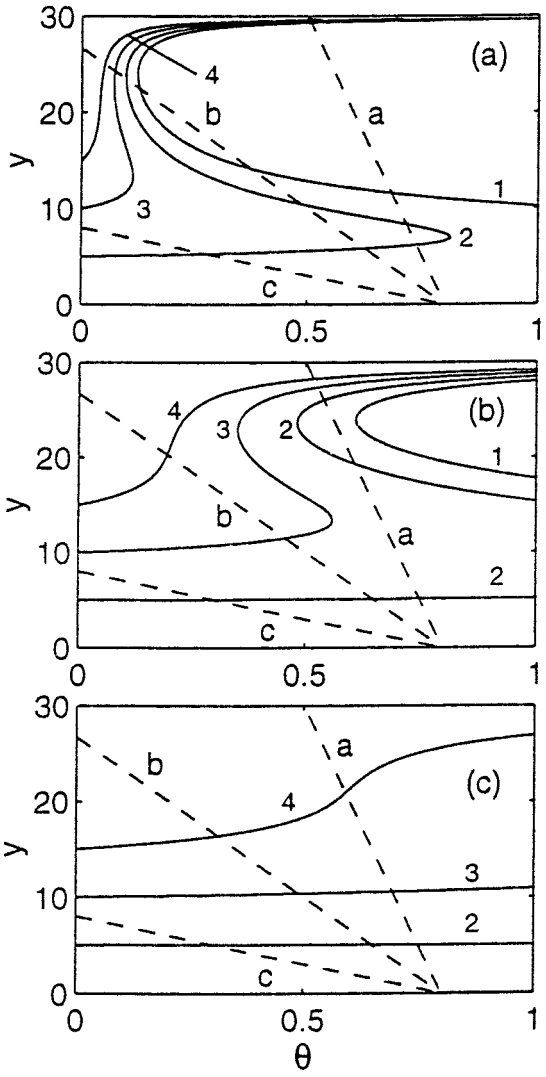


**Figure 4. Typical approximate phase-planes in an adiabatic reactor.**

$Pe_T = 100$ (a), 500 (b), and 1,500 (c), showing the enthalpy and activity null curves ($f = 0$ and $g = 0$) with $B = 30$, $\gamma = 20$, $Da = 0.06$, $K = 4.0$; $M = 1$, 3 or 10 for lines $a$, $b$, $c$, respectively; $y^* = 0$, 5.0, 10.0 and 15.0 for lines 1–4, respectively).

process of a solid–solid noncatalytic reaction, which is mathematically quite similar to the problem of interest. In the case of fixed activity ($\theta = 1$) and with $Pe_C \to \infty$, the front velocity, assuming complete conversion across the front and large activation energies, was shown to be $(V-1)^2 = Dae^{y+}/(BPe_T)$, for a front that connects the $y = 0$ and $y = y_+$ states; in the original coordinate system, and for an adiabatic temperature rise ($y_+ = B$), that implies

$$V = -\sqrt{\frac{Dae^B}{BPe_T}} + 1. \qquad (19)$$

The front velocity depends on activity (i.e., $Da$) and it is biased for motion in the flow direction. This result applies mainly to the wave formed upon the ignition of a cold bed, with a minus sign in front of the root term: such a front will propagate downstream for low $Dae^B$ terms and upstream for highly active states. The front may loose stability via a Hopf bifurcation and propagate with an oscillatory amplitude (Matkowsky and Sivashinsky, 1978); the boundary of that instability was approximated, assuming an infinitely narrow reaction zone.

### *Model simulations*

Model simulations in its dimensionless form (Eqs. 12 and 13) were conducted as explained earlier. The results below present typical motions for relatively large $Pe_T$ numbers ($>50$), conditions that induce sharp fronts, along with the transitions from stable to oscillatory motion. We employed either large (10) or small (0.1) ratios of $Pe_C/Pe_T$, but show that this parameter does not affect the qualitative behavior.

Simulations of adiabatic reactors with a high $Pe_C/Pe_T$ ratio (10 in the simulations below), showed the following types of solutions:

1. A fully ignited or a fully extinguished state exists at very low or very high $M$ values, respectively, as expected from phase-plane analysis: for low $M$ values, the phase planes spanned by the system are bistable at low $y^*$ and single-valued ignited at large $y^*$. Part of this domain is excitable, as described below (4).

2. A stationary front emerges at low $M$ and high $Pe_T$ values (shown in Figure 5a, with $Pe_T = Pe_C/10 = 1500$, for $M = 0.1$, for which the inlet is extinguished); for higher $M$ it changes into an oscillatory front motion (Figures 5b and 5c). With increasing $M$ the front position is shifted toward the exit and its amplitude grows (Figure 5). The transition from the fully ignited to the fully extinguished state, upon varying $M$, occurs at high $Pe_T$ through intermediate states with a stationary or oscillatory front (as shown in Figure 5).

3. Oscillatory motions with fronts that span the whole surface emerge for intermediate $M$ values at lower $Pe$ numbers (Figure 6; $Pe_T = Pe_C/10 = 100$). The fast extinction front travels downstream while the ignition front moves upstream. With increasing $M$ the ignited zones of the temporal oscillations diminish while the extinguished sections broaden, as ex-

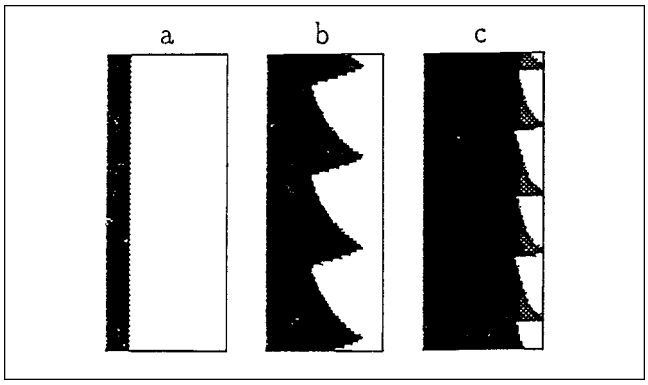


**Figure 5. Transition in an adiabatic reactor from an ignited to an extinguished state through a stationary state and oscillatory front.**

(a) $M = 0.1$; (b) $M = 1$; (c) $M = 4.35$ with $Pe_T = 1{,}500$, $Pe_C = 15{,}000$, $B = 30$, $\gamma = 20$, $Da = 0.06$, $Le^* = 100$, $\tau_\theta = 1{,}000$, $K = 4$.

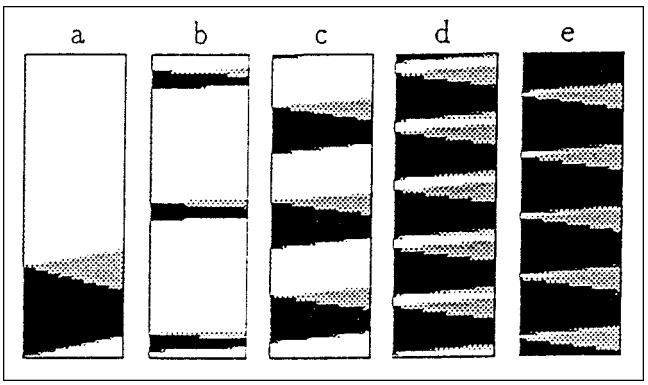


**Figure 6. Transition in an adiabatic reactor from an ignited to an extinguished state through oscillatory states.**

(b–e: $M = 2.77$, 2.8, 5, and 11) with $Pe_T = 100$, $Pe_C = 1{,}000$; other parameters as in Figure 5; part (a) presents the response to a perturbation in an excitable state ($M = 2.7$; see also Figure 7a).

pected from relaxation oscillations. Note that for these $M$ values the system spans an oscillatory phase plane that triggers the reactor dynamics.

The spatial profiles of one such oscillatory state (Figure 7c), and the corresponding temporal pattern of the inlet and outlet temperatures (lines 1 and 2, Figure 7d) exhibit four sections: (a) initially the reactor is extinct and exhibits a slow activation process; the concentration and temperature are adiabatically related ($y = Bx$, compare solid and broken lines). (b) A front is formed at the exit and travels upstream at an apparently constant speed. The temperature behind the front falls below the adiabatic temperature rise ($B$), but the conversion is complete. (c) The front disappears at the inlet, the reactor is ignited, and it deactivates slowly. (d) A front is formed at the inlet and travels downstream, showing some acceleration. The temperature behind the front exceeds $B$.

To account for the temperature behind a front that travels at a constant speed ($V$), we use the transformation $\zeta = \xi - V\tau$ to convert the mass and enthalpy balances (Eq. 12) and subtract them to eliminate the reaction term. We find that

$$I \equiv Bx - y - V(Bx - Ley) - \frac{\partial(Bx/Pe_C - y/Pe_T)}{\partial\zeta}, \quad (20)$$

is invariant, that is, $\partial I/\partial\zeta = 0$, and $I$ is a constant and its value can be estimated at the inlet, where $x = y = 0$ and gradients are small, $I = 0$. The temperature behind the front, where conversion is complete ($x = 1$) and gradients are small, is

$$y_+ = B(1-V)/(1-LeV). \quad (21)$$

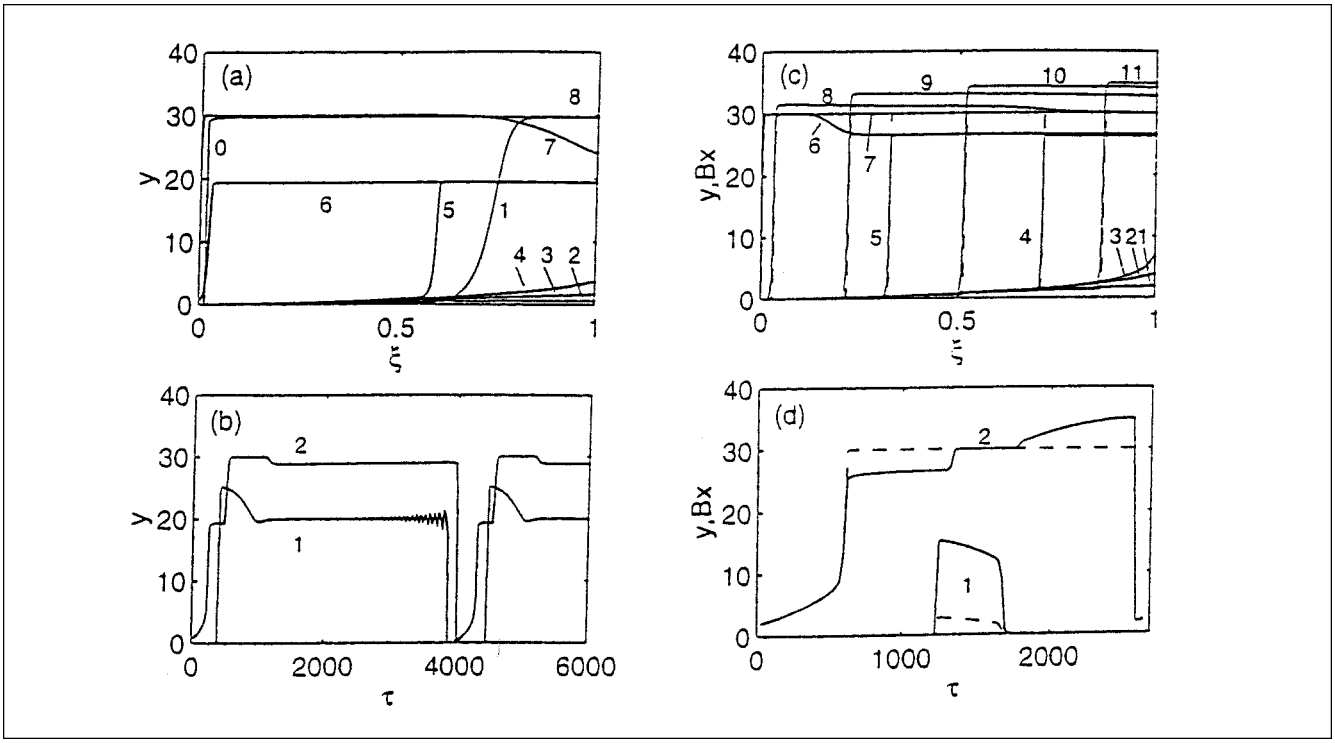


**Figure 7. (a) Spatial behavior of an excitable state upon a perturbation at the inlet ($M = 2.7$ parameters as in Figure 6a; lines are equally intervaled); (b) temporal behavior of inlet and outlet temperatures of an oscillatory state, close to the point of infinite-period bifurcation ($M = 2.77$, parameters as in Figure 6b); (c,d) spatial and temporal behavior of temperature ($y$, solid line) and concentration ($x$, broken) during an oscillatory cycle.**

($Pe_T = Pe_C/10 = 500$, $Da = 0.05$, $M = 2$, other parameters as in Figure 6; in (c) lines are equally intervaled; in (d) lines 1 and 2 in (d) denote inlet and outlet conditions, respectively).

Thus, temperatures behind the front exceed (fall below) $B$ when the front moves downstream (upstream). The temperature–concentration relation at intermediate positions depends on their gradients.

4. The ignited solution may be perturbed and excited. Let us review this motion in the reaction–conduction system and then study the effect of convection. Excitable media are extended nonequilibrium systems having homogeneous rest states that are linearly stable but susceptible to finite perturbations. Triggering the edge of an excitable system will send a front traveling at constant speed. After a certain period the perturbed position will relax, undergo an opposite transition, and will send a second front in the direction of the leading one. Eventually, in a sufficiently long system, the two fronts will form a pulse, traveling at a constant speed and shape. Excitable media also support continuous families of periodic wave trains when the system is triggered continuously. Returning now to the homogeneous model with convection we induce a local extinction at the reactor inlet of an ignited and excitable state ($M = 2.7$, line 0 in Figure 7a): it produces a downstream-propagating extinction front that exits the system and leaves it cold; subsequent spontaneous ignition occurs at the exit and creates an upstream-moving front that restores the original state (line 8; lines are plotted with fixed time-intervals). Note again that the temperature behind the front is lower than $B$. The upstream-propagating front is slower than that moving downstream. This is also evident from the contour plot (Figure 6a). Excitation induced at the reactor exit did not propagate in this case (not shown).

5. The transition from an ignited-excitable to an oscillatory state occurs at $M = 2.77$ for the parameters of Figure 6, through an infinite-period bifurcation (homoclinic orbit), composed here from relaxation oscillations with a growing-amplitude motion along the upper segment (see one temporal cycle in Figure 7b).

The effect of the $Pe$ number is demonstrated in Figure 8. As expected from the phase-plane analysis, the amplitude of oscillations in the front position declines with increasing $Pe_T$, and eventually the oscillations disappear for sufficiently high $Pe_T$.

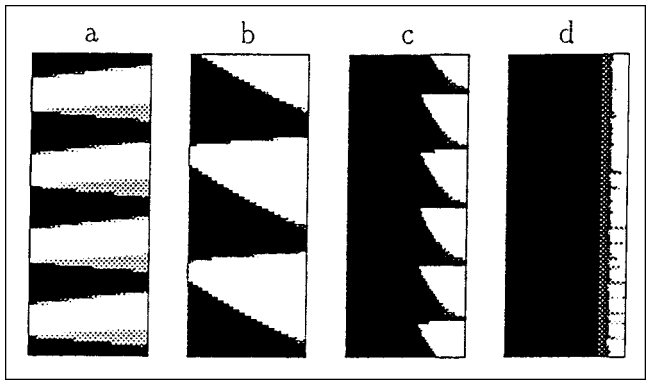


**Figure 8. Effect of $Pe_T$ on the behavior of an adiabatic bed: (a-d: $Pe_p$ = 50, 500, 1,500, 5,000).**

$Pe_T = Pe_C/10$, $Da = 0.06$, $M = 4$, $K = 3.0$; other parameters as in Figure 5.

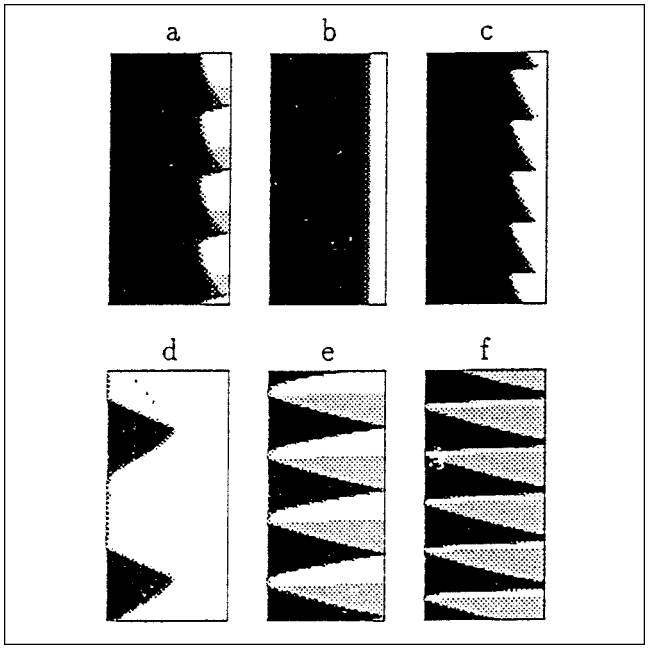


**Figure 9. Transition from an ignited to an extinguished state through a stationary or oscillating front (states b–c: $M$ = 2.0 or 3.0, respectively, $Pe_T$ = 100, $\tau_\theta = 10^2$), or through oscillatory states (d–f: $M$ = 1.75, 2, and 3, respectively, $Pe_T$ = 50, $\tau_\theta = 10^3$), in an adiabatic reactor.**

$Pe_T/Pe_C = 10$; other parameters as in Figure 5, (Parts (a) and (b) were simulated under the same conditions with $\tau_\theta = 10^3$ or $10^2$, respectively).

Similar observations were made with $Pe_C/Pe_T = 0.1$. At very low or very high $M$ values, the state is ignited or extinguished, respectively; the transition occurs through stationary- and oscillatory-front solutions at $Pe_T = 100$ or larger (Figures 9b and 9c), or through an oscillatory motion that sweeps the whole surface at $Pe_T = 50$ or lower (Figures 9d–9f). Increasing the ratio of time scales will also convert a stationary front into an oscillatory one (compare Figures 9a and 9b). Increasing the reactor length (not shown) will push the system into an oscillatory phase plane at lower $M$ values, but will not affect the sequence of patterns.

In a nonadiabatic reactor the temperature profile exhibits a sharp front upstream and a relaxation to $y_w$ downstream. In a typical oscillatory motion the hot spot travels back and forth within the reactor while maintaining qualitatively the same shape of a sharp front and moderate cooling zone ($\alpha_T = 1.0$; Figure 10). The contour plot is quite similar in lower $\alpha_T$ values (Figure 11), in which the front sweeps the whole surface, except that the cooling zone becomes more moderate and, of course, the profile becomes monotonic with $\alpha_T = 0$. The motion just described for $\alpha_T = 1$ is qualitatively maintained for $\alpha_T < 1.18$, and then turns into a stationary front that is maintained for $1.2 < \alpha_T < 7.0$ (see Figure 10e). The state is extinguished for larger values. The latter state coexists with the oscillatory or with the stationary front solutions mentioned earlier, in the range $1 < \alpha_T < 7$.

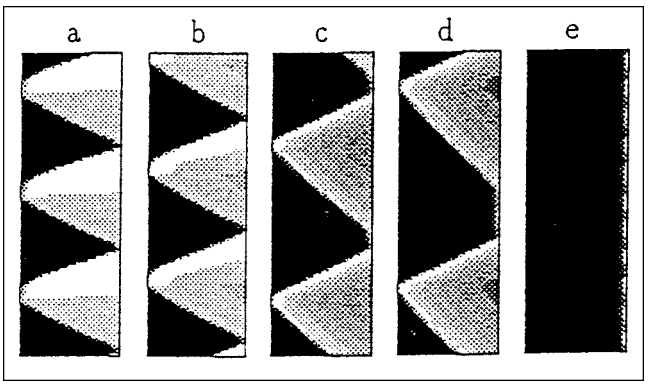


**Figure 10. Oscillatory behavior in a nonadiabatic reactor.**

$\alpha_T = 0$ (a: adiabatic), 0.2 (b), 1.0 (c), 1.18 (d), and 1.2 (e); $M = 2.0$, $Pe_T = Pe_C/10 = 50$; other parameters as in Figure 5.

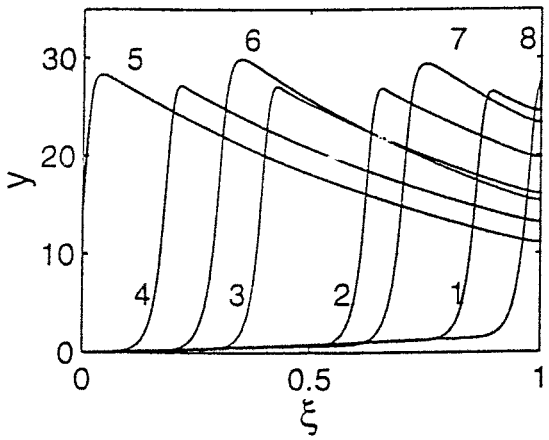


**Figure 11. Temporal behavior of the state in Figure 10c.**

## Concluding Remarks

Pattern formation mechanisms have been analyzed for the homogeneous model of a fixed catalytic bed for reactions with oscillatory kinetics. Two cases were analyzed: a nonadiabatic reactor with a continuous mass-supply (either by the preceding reaction or via the membrane wall), and a simple adiabatic or cooled reactor. In the former case the system may reach asymptotic space-independent solutions, and when bistability of such solutions exists, fronts separating different steady states may be established. In that case, we showed that the front velocity is linearly dependent on the fluid velocity so that upstream propagating fronts are slow or impossible, while propagation downstream is fast. Stationary or oscillatory front solutions, oscillatory states that sweep the whole surface or excitation fronts, may be realized then, and the reactor behavior can be predicted from the sequence of phase-planes spanned by the reactor. In an adiabatic reactor, fronts are formed only for sufficiently small $Pe_p$ numbers (yet, the critical $Pe_p$ is large for highly exothermic and highly activated reactions). These frontlike solutions do not separate different steady states. The patterns that can be realized in this case are quite similar to those in the previous case. The reactor behavior can be predicted by the sequence of phase planes spanned by the reactor, using an approximate finite difference presentation that converts the convection term into a supply term.

These two types of fronts should be compared with fronts in a heterogeneous reactor model and with fronts in a uniform medium. As noted in the Introduction, pattern-forming mechanisms are somewhat different in homogeneous- and heterogeneous-reactor models. Heterogeneous models are typically defined by the existence of temperature and concentration gradients between the solid and fluid phases. This is a quantitative, rather than a qualitative, criterion, and it fails to demonstrate the expected differences. When the steady-state solution of the solid phase is single-valued for all fluid-phase conditions spanned by the reactor, then its (numerical or analytical) solution can be substituted into the fluid phase and, in that case, at least at steady state, there is no significant qualitative difference between the two classes of models. In a truly heterogeneous model the solid-phase solution is not single-valued, and thus it cannot be lumped. Fronts in the heterogeneous model separate different local solid-phase steady states, which, in turn, depend on gradients on the fluid phase. Now we note the differences between the patterns in these systems:

- Fronts and patterns in the homogeneous model of an adiabatic reactor disappear for sufficiently large $Pe_T$ numbers, while in the heterogeneous model they persist (as long as significant interphase gradients persist). As we show in a forthcoming article, for small interphase resistances, patterns in the heterogeneous model can be predicted with a homogeneous one using an effective $Pe_p$ number.
- Patterns in a nonadiabatic reactor persist for sufficiently small cooling rates and disappear for fast cooling as the reactor becomes almost isothermal. In the heterogeneous model, on the other hand, under strong cooling rates (yet, when reaction persists) the system may exhibit even a richer class of patterns due to the interaction of convection and reaction. If an ignition occurs at the reactor inlet under these conditions, it will likely cause extinction at the reactor exit, due to reactant consumption. In an adiabatic reactor, on the other hand, local ignition at the inlet will increase the fluid temperature downstream and will induce an ignition there as well (see Shvartsman and Sheintuch, 1995).

## Acknowledgment

Work supported by the U.S.-Israel Binational Science Foundation and by the Technion V.P.R. Fund-Promotion of Sponsored Research. MS is a member of the Minerva Center of Nonlinear Dynamics and Complex Systems. One of the authors (O.N.) is supported by the Ministry of Absorption. The CRE group is supported by the DuPont Educational Aid Fund.

## Notation

$A_v$ = interphase surface area per reactor volume
$B$ = dimensionless exothermicity
$C_A, C_{Af}$ = key component concentration in solid and fluid phase, respectively
$D_e$ = effective axial dispersion coefficient
$Da$ = Damkohler number
$E$ = activation energy
$f, g$ = kinetic functions

$h$ = interphase heat-transfer coefficient
$\Delta H$ = reaction enthalpy
$H, H_C$ = wall-to-fluid heat- and mass-transfer coefficients
$K$ = deactivation parameter
$k_{d+}$, $k_{d-}$ = activation and deactivation rate constants
$k_g$ = mass-transfer coefficient
$k_w$ = catalytic reaction-rate preexponential constant
$k_e$ = effective axial conductivity
$Le^*$ = Lewis number; the ratio of solid-to-fluid-phase heat capacities
$M$ = deactivation parameter
$Pe_T$, $Pe_C$ = Peclet numbers for heat and mass dispersion
$r$ = reaction rate
$U$ = scaled fluid velocity (Eq. 6, equal to thermal-front velocity due to convection and reaction)
$u_s$ = interstitial fluid velocity
$t$ = time
$T, T_f$ = solid and fluid temperature, respectively
$x$ = dimensionless concentration
$z, \zeta$ = dimensional and dimensionless axial coordinate
$\alpha_C$, $\alpha_T$ = dimensionless fluid-to-wall transport coefficient
$\gamma$ = dimensionless activation energy
$\Delta T_{\text{ad}}$, $\Delta T_x$ = adiabatic temperature rise, temperature rise due to external resistance
$\epsilon$ = bed void fraction
$\rho c_{pf}, \rho_s c_{ps}$ = volume-specific heat capacity of the fluid and solid phases
$\theta$ = activity
$\tau$ = dimensionless time

### *Subscripts*

$e, i$ = value at ignition and extinction, respectively
$C, T, \theta$ = of the respective variables
$s$ = at steady state

## Literature Cited


Balakotayah, V., "Structural Stability of Nonlinear Convection-Reaction Models," *Chem. Eng. Educ.*, **30**, 234 (1996).

Barto, M., and M. Sheintuch, "Excitable Waves and Spatiotemporal Patterns in a Fixed-Bed Reactor," *AIChE J.*, **40**, 120 (1994).

Fife, P. C., *Mathematical Aspects of Reacting and Diffusing Systems*, Springer-Verlag, Berlin (1979).

Frank-Kamenetskij, D. A., *Diffusion and Heat Transfer in Chemical Kinetics*, 2nd ed., Plenum Press, New York (1969).

Hlavacek, V., and O. Van Rompay, "Current Problems of Multiplicity, Stability and Sensitivity of States in Chemically Reacting Systems," *Chem. Eng. Sci.*, **36**, 1587 (1981).

Imbihl, R., and G. Ertl, "Oscillatory Kinetics in Heterogeneous Catalysis," *Chem. Rev.*, **95**, 697 (1995).

Luss, D., "Temperature Fronts and Patterns in Catalytic Systems," *Ind. Eng. Chem. Res.*, **36**, 2931 (1977).

Matkowsky, B. Y., and G. I. Sivashinsky, "Propagation of a Pulsating Reaction Front in Solid Fluid Combustion," *SIAM J. Appl. Math.*, **35**, 465 (1978).

Merzhanov, A. G., A. K. Filomenko, and I. P. Borovinskaja, *Dokl. Akad. Nauk SSSR*, **208**, 892 (1973).

Middya, U., D. Luss, and M. Sheintuch, "Spatiotemporal Motions Due to Global Interaction," *J. Chem. Phys.*, **100**, 3568 (1994).

Mikhailov, A. S., *Foundations of Synergetics, I. Distributed Active Systems*, Springer-Verlag, Berlin (1991).

Puszynski, J., J. Degreve, and V. Hlavacek, "Modeling of Exothermic Solid-Solid Noncatalytic Reactions," *Ind. Eng. Chem. Res.*, **26**, 1424 (1987).

Rovinsky, A. B., and M. Menzinger, "Chemical Instability Induced by a Differential Flow," *Phys. Rev. Lett.*, **69**, 1139 (1992).

Rovinsky, A. B., and M. Menzinger, "Self-Organization Induced by Differential Flow of Activator and Inhibitor," *Phys. Rev. Lett.*, **70**, 778 (1993).

Schuth, F., B. E. Henry, and L. D. Schmidt, "Oscillatory Reactions in Heterogeneous Catalysis," *Adv. Catal.*, **39**, 51 (1993).

Sheintuch, M., "Spatiotemporal Structures of Controlled Catalytic Wires," *Chem. Eng. Sci.*, **44**, 1081 (1989).

Sheintuch, M., and S. Shvartsman, "Patterns Due to Convection-Conduction-Reaction Interaction in a Fixed-Bed Catalytic Reactor," *Chem. Eng. Sci.*, **49**, 5315 (1994).

Sheintuch, M., and S. Shvartsman, "Spatiotemporal Patterns in Catalytic Reactors," *AIChE J.*, **42**, 1041 (1996).

Shvartsman, S., and M. Sheintuch, "One- and Two-Dimensional Spatiotemporal Thermal Patterns in a Fixed-Bed Reactor," *Chem. Eng. Sci.*, **50**, 3125 (1995).

Slinko, M. M., and N. I. Jaeger, *Oscillating Heterogeneous Catalytic Systems*, Elsvier, Amsterdam (1994).

Subramanian, S., and V. Balakotaiah, "Classification of Steady-State and Dynamic Behavior of Distributed Reactor Models," *Chem. Eng. Sci.*, **51**, 401 (1996).

Wicke, E., and H. U. Onken, "Periodicity and Chaos in a Catalytic Packed Bed Reactor for CO Oxidation," *Chem. Eng. Sci.*, **43**, 2289 (1998).

Wicke, E., and D. Vortmeyer, "Zudzonen heterogener Reaktionen in gasdurchstromten Kornerschichten," *Z. Elektochem. Ber. Bunsenges. Physik. Chem.*, **63**, 145 (1959).

Zeldovich, Yu. B., and G. I. Barenblatt, "Theory of Flame Propagation," *Combus. Flame*, **2**, 61 (1959).



*Manuscript received June 24, 1998, and revision received Nov. 12, 1998.*